Kinetic Characterization of Protein Arginine Deiminase 4: A Transcriptional Corepressor Implicated in the Onset and Progression of Rheumatoid Arthritis†

Patricia L. Kearney,‡,§ Monica Bhatia,‡,§ Nelroy G. Jones,§ Luo Yuan,§ Mary C. Glascock,§ Kristen L. Catchings,§ Michiyuki Yamada,‖ and Paul R. Thompson*,§,⊥

Department of Chemistry and Biochemistry, University of South Carolina, 631 Sumter Street, and University of South Carolina Nanocenter, Columbia, South Carolina 29208, and Graduate School of Integrated Science, Yokohama City University, Yokohama, Japan

Received February 17, 2005; Revised Manuscript Received May 18, 2005

ABSTRACT: Protein arginine deiminase 4 (PAD4) is a Ca^{2+}-dependent enzyme that catalyzes the posttranslational conversion of arginine to citrulline (Arg → Cit) in a number of proteins, including histones. While the gene encoding this enzyme has been implicated in the pathophysiology of rheumatoid arthritis (RA), little is known about its mechanism of catalysis, its in vivo role, or its role in the pathophysiology of RA; however, recent reports suggest that this enzyme can act as a transcriptional corepressor for the estrogen receptor. Herein, we report our initial kinetic and mechanistic characterization of human PAD4. Specifically, these studies confirm that PAD4 catalyzes the hydrolytic deimination of Arg residues to produce Cit and ammonia. The metal dependence of PAD4 has also been evaluated, and the results indicate that PAD4 activity is highly specific for calcium. Calcium activation of PAD4 catalysis exhibits positive cooperativity with $K_{0.5}$ values in the mid to high micromolar range. Evidence indicating that calcium binding causes a conformational change is also presented. Additionally, the steady-state kinetic parameters for a number of histone H4-based peptide substrates and benzoylated Arg derivatives have been determined. K_m values for these compounds are in the high micromolar to the low millimolar range with k_{cat} values ranging from 2.8 to 6.6 s^{-1}. The ability of PAD4 to catalyze the deimination of methylated Arg residues has also been evaluated, and the results indicate that these compounds are poor PAD4 substrates ($V/K \leq 31.3\ M^{-1}\ s^{-1}$) in comparison to other substrates. These findings suggest that the full-length enzyme does not catalyze this reaction in vitro and possibly in vivo either. Collectively, the studies described herein will provide a firm foundation for the future development of PAD4 selective inhibitors.

Protein arginine deiminases (PADs)[1] are a group of calcium-dependent vertebrate enzymes that catalyze the posttranslational conversion of arginine to citrulline (Arg → Cit) in a variety of different proteins (Figure 1). Recently, PAD research has come into focus because the gene encoding PAD4 has been suggested as a susceptibility locus for rheumatoid arthritis (RA) in the Japanese population (*1*). While a conclusive link between PAD4 and RA in French, German, and English populations has yet to be demonstrated (*2*−*4*), the preponderance of evidence from serological and biochemical studies suggests that PAD activity, in general, plays a role in the onset and progression of RA (*5*−*17*). These data include the fact that the RA-associated HLA-DRB1*0401 MHC class II molecule binds with high affinity to a Cit-containing peptide (*17*). While the precise role of PAD4, and/or other PADs [e.g., PAD2 (*5*)], in the pathophysiology of RA is largely speculative, studies suggest that an elevated PAD activity is disease-causing in at least a subset of the patient population.

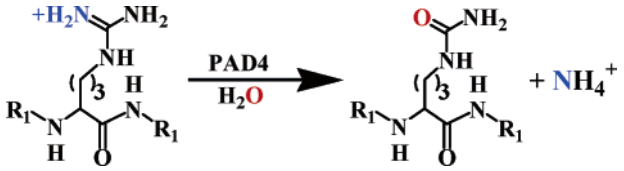

FIGURE 1: Reaction catalyzed by PAD4. R_1 = substrate protein sequences.

The finding that PAD4 catalyzes the deimination of histones H2A, H3, and H4 (*18*, *19*) has also drawn the attention of a broader community of scientists who are interested in characterizing the role of histone modifications in regulating gene transcription. In fact, Kouzarides, Coonrod, Allis, and their colleagues have recently demonstrated that PAD4 acts as a transcriptional corepressor of estrogen receptor signaling and that the ability of PAD4 to alter gene transcription is peculiar to its catalytically active form (*20*, *21*).

† This work was supported in part by start-up funds from the University of South Carolina Research Foundation (to P.R.T.).

* To whom correspondence should be addressed at the Department of Chemistry and Biochemistry, University of South Carolina. Tel: (803) 777-6414. Fax: (803) 777-9521. E-mail: Thompson@mail.chem.sc.edu.

‡ These authors contributed equally to this work.

§ University of South Carolina.

‖ Yokohama City University.

⊥ University of South Carolina Nanocenter.

[1] Abbreviations: PAD, protein arginine deiminase; Cit, citrulline; RA, rheumatoid arthritis; BAEE, benzoyl-L-arginine ethyl ester; BAME, benzoyl-L-arginine methyl ester; BA, benzoyl-L-arginine; BAA, benzoyl-L-arginine amide; DTT, dithiothreitol; MMA, monomethylarginine; ADMA, asymmetric dimethylarginine.

10.1021/bi050292m CCC: $30.25
Published on Web 07/09/2005

PAD4 is a 663 amino acid, 74 kDa, protein that was initially identified as a protein whose expression was induced in HL-60 cells treated with differentiating agents (*22*). However, beyond the research discussed above, little is known about PAD catalysis, substrate specificity, regulation, or in vivo role. In fact, the entire PAD family of enzymes has been poorly characterized at the *molecular* level; and while partial enzymatic characterizations of nonhuman PAD isoforms purified from various tissue sources were performed in the 1970s and 1980s (e.g., rat epidermis, bovine brain, rabbit skeletal muscle, and guinea pig hair follicles) (*23*−*27*), these studies failed to address the molecular mechanisms of catalysis, substrate recognition, regulation, and in vivo roles of these enzymes using highly purified enzyme preparations. Furthermore, even though the three-dimensional structure of PAD4 is known (*28*), detailed molecular characterizations of human PAD catalysis, substrate recognition, and regulation have not been performed.

To begin to redress these deficiencies, we and others (*29*) have initiated studies to quantitatively characterize PAD4 activity using purified recombinant enzyme. The information derived from these studies is expected to aid the design and synthesis of PAD4 selective inhibitors that can be used to study the role of histone deimination in physiologically relevant pathways [e.g., estrogen receptor regulated transcription (*20*, *21*)], as well as the role of this enzyme in the onset and progression of RA. The development of such pharmacological tools is important because the in vivo role of PAD4, and other human PADs, is poorly defined. This is especially true with regard to their putative role in cell signaling.

MATERIALS AND METHODS

Chemicals. *N*-α-Benzoyl-L-arginine ethyl ester (BAEE), dithiothreitol, HEPES, glutathione, ammonium iron(III) sulfate dodecahydrate, and Trizma−HCl were acquired from Sigma (St. Louis, MO). *N*-α-Benzoyl-L-arginine methyl ester (BAME) and N^G-methyl-L-arginine acetate were obtained from MP Biomedicals (Irvine, CA). N^G,$N^{G\prime}$(symmetric)-dimethyl-L-arginine dihydrochloride and N^G,N^G(asymmetric)-dimethyl-L-arginine dihydrochloride were obtained from Calbiochem (San Diego, CA). Pbf-protected Fmoc-monomethyl-L-Arg and Fmoc-N^G,N^G(asymmetric)-dimethyl-L-Arg were obtained from EMD Biosciences (Darmstadt, Germany) and BACHEM (King of Prussia, PA), respectively. Glutathione−Sepharose and PreScission protease were purchased from Amersham Biosciences (Piscataway, NJ). Diacetyl monooxime (DAMO), *N*-α-benzoyl-L-arginine (BA), and *N*-α-benzoyl-L-arginine amide (BAA) were obtained from Acros (Hampton, NH). Thiosemicarbazide was procured from Aldrich (Milwaukee, MI), and [^{18}O]water (95%) was obtained from Cambridge Isotopes (Andover, MA). The anti-modified Cit antibody was from Upstate Cell Signalling (Lake Placid, NY).

Purification of PAD4. To characterize the molecular mechanism of PAD4, a recombinant human PAD4 *Escherichia coli* expression system was obtained from the Yamada group. This expression system (*22*) encodes full-length PAD4 with an 8-residue N-terminal linker that is fused in frame to a PreScission protease cleavable GST tag. The predicted molecular mass of PAD4 including this 8-residue linker is 74879 g/mol. The PAD4 expression construct was transformed into *E. coli* Rosetta cells (EMD Biosciences) for protein expression. The GST-PAD4 purification procedure described herein was adapted from previously described methods (*30*). Briefly, overnight cultures were used to inoculate 4 × 2 L of 2YT [16 g/L bacto-tryptone, 10 g/L bacto-yeast extract, and 5 g/L NaCl], and these cultures were grown at 37 °C and 220 rpm until the cultures reached an OD_{600} of 0.6. PAD4 expression was induced by the addition of IPTG (0.5 mM final) and allowed to proceed overnight at 16 °C and 220 rpm. Cells were harvested by centrifugation at 5000 rpm for 10 min at 4 °C. The pellet was resuspended in 70 mL of lysis buffer (20 mM Tris-HCl, pH 8.0, 1 mM EDTA, 1 mM DTT, 10% glycerol, and 0.5 mM PMSF) and lysed by five cycles of sonication (duty cycle 50%, output 4). The supernatant was immediately applied to a glutathione−Sepharose column preequilibrated with low salt buffer (20 mM Tris-HCl, pH 8.0, 1 mM EDTA, 1 mM DTT, 10% glycerol, and 200 mM NaCl). Initial binding was carried out for 10 min at 4° C with gentle rocking. The column was washed with 50 mL of low salt buffer, followed by 50 mL of high salt buffer (20 mM Tris-HCl, pH 8.0, 1 mM EDTA, 1 mM DTT, 10% glyercol, and 500 mM NaCl). Beads were resuspended in roughly 15 mL of low salt buffer, and 30 μL of PreScission protease was added to perform an on-column cleavage reaction (16 h at 4 °C). PAD4 was eluted with 75 mL of low salt buffer, and 25 mL fractions were collected.

Fractions containing PAD4 activity were applied to a Mono Q HR5/5 strong anion-exchange column (Amersham Biosciences) preequilibrated with 20 mM Tris-HCl, pH 8.5. A linear gradient of 0−100% buffer B (20 mM Tris-HCl, pH 8.5, plus 1 M NaCl) was used to further purify full-length GST-cleaved PAD4. The flow rate was 0.5 mL/min, and 2 mL fractions were collected. Fractions from the Mono Q were analyzed by SDS−PAGE and PAD activity assays (see below for details). Fractions containing pure full-length PAD4 were pooled and concentrated using a Centricon concentrator (Millipore Corp., Bedford, MA) with a 10 kDa nominal molecular mass cutoff. Concentrated protein was then dialyzed (20 mM Tris-HCl, pH 8.0, 1 mM EDTA, 500 mM NaCl, 1 mM DTT, and 10% glycerol), flash frozen in liquid nitrogen, and stored at −80 °C. PAD4 stored in this manner was stable for several months.

^{18}O Studies. ^{18}O incorporation into BAEE was assayed by performing large-scale PAD4-catalyzed deimination reactions in either normal or ^{18}O-labeled water. For these experiments, PAD4 (0.2 μM final) was incubated at 37 °C in a reaction buffer containing 5 mM BAEE, 50 mM Tris-HCl, pH 7.6, 10 mM $CaCl_2$, 5 mM DTT, and 50 mM NaCl. The reaction buffer was made with either normal or ^{18}O-labeled water. For the ^{18}O experiments, the mole percentage of ^{18}O-labeled water was 73% final. After 3 h of incubation, the reaction mixture was desalted, using a C18-Zip tip (Millipore), per the manufacturer's instructions, at which point the deiminated product was analyzed by ESI mass spectrometry using a Waters Micromass quadrupole-time-of-flight (Q-TOF) tandem mass spectrometer in the positive ion mode. Formic acid (0.1%) was used as the organic modifier.

Kinetic Assay. The PAD4 assay carried out in this study has essentially been described previously (*31*). Briefly, this is a discontinuous colorimetric assay that measures the formation of ureido-containing compounds i.e., Cit, urea,

methylurea, etc. Steady-state kinetic parameters were determined with variable amounts of the benzoylated Arg derivatives in a reaction buffer containing 100 mM Tris-HCl, pH 7.6, 50 mM NaCl, 2 mM DTT, and 10 mM $CaCl_2$ (60 μL final volume). TRIZMA base, minimum 99.9% titration, was used for kinetic studies to minimize the presence of contaminating metal ions in the assay buffer. The trace element composition of the buffer solutions was measured by ICP-AES with a Perkin-Elmer Plasma 400 (Perkin-Elmer, Norwalk, CT), using aqueous standards (High-Purity Standards, Charleston, SC) and a three-point calibration graph. The concentrations of barium, manganese, magnesium, and strontium were all below the limit of detection, approximately 0.01 μM. Calcium, samarium, and zinc were detectable, but their concentrations were less than 0.15 μM. Thus, the starting concentrations of metal ions in our solutions do not make a significant contribution to their final assay concentrations, which are in the high micromolar to millimolar range.

The reaction mixtures described above were preincubated for 10 min at 37 °C, at which point PAD4 was added to a final concentration of 0.2 μM to initiate the reaction. Reactions were quenched by flash freezing in liquid nitrogen. For color development, 200 μL of freshly prepared COLDER solution [2.25 M H_3PO_4, 4.5 M H_2SO_4, 1.5 mM $NH_4Fe(SO_4)$, 20 mM diacetyl monoxime, and 1.5 mM thiosemicarbazide] was added to the quenched reaction, vortexed to ensure complete mixing, and then incubated for 30 min at 95 °C. The absorbance at 540 nm was then measured and compared to a Cit standard curve to determine the concentration of Cit produced during the course of the reaction.

All kinetic studies were performed in the linear range of PAD4 activity with respect to time and enzyme concentration. Assays were performed in duplicate, and agreement within 20% was required for inclusion in this study. The initial rates obtained from these experiments were fit to eq 1, using the Kaleidagraph version 3.09 software package.

$$v = V_{max}[S]/(K_m + [S]) \quad (1)$$

pH Dependence. The pH dependence of PAD4 was characterized under pseudo-*V/K* conditions. Briefly, the ability of PAD4 to deiminate BAEE (1 mM final concentration) was evaluated over a broad pH range (pH 4.5−9.0), using a multicomponent buffering system containing 50 mM Tris-HCl/50 mM Bis-Tris/100 mM sodium acetate, 50 mM NaCl, 2 mM DTT, and 10 mM $CaCl_2$. Assays were preincubated for 10 min at 37 °C, at which point PAD4 (0.2 μM final concentration) was added to initiate the reaction. The rates obtained from these experiments were plotted versus pH and fit to eq 2, using the Kaleidagraph version 3.09 software package.

$$\log(k_{cat}/K_m)_{app} = \log[k_{cat}/K_m(1 + H/K_1 + K_2/H)] \quad (2)$$

The time course of BAEE deimination (10 mM final) was also evaluated at the indicated pH values to ensure that the loss of activity associated with the pH changes was due to a change in the protonation state of the enzyme and not due to pH-induced denaturation of the enzyme. Cit production was measured using the methodology outlined for the kinetic assay.

Ammonia Production. Ammonia production was verified by performing time course experiments and measuring both the ammonia and the Cit produced. BAEE was used as the substrate (10 mM final) in a reaction buffer containing 100 mM HEPES, pH 8.0, 50 mM NaCl, 2 mM DTT, and 10 mM $CaCl_2$. After a 10 min preincubation of the reaction buffer and substrate at 37 °C, PAD4 (0.2 μM) was added to initiate the reaction. Aliquots of 60 μL were removed from the reaction mixture at 0, 2, 4, 6, 10, and 15 min after the initiation of the reaction. The reaction was quenched by the addition of 3 volumes of 50 mM EDTA. Concentrations of ammonia were determined by the fluorometric method of Sugawara and Oyama (*32*). Cit production was measured in parallel using the methodology outlined above for the kinetic studies.

Calcium Dependence. The calcium dependence of PAD4 was determined at or near saturating concentrations ($>5K_m$) for all substrates (10 mM final) except BA. The calcium dependence of this substrate was determined at 5 mM because of solubility issues associated with this substrate. Reactions were performed in assay buffer containing 100 mM Tris-HCl, pH 7.6, 50 mM NaCl, 2 mM DTT, and varying concentrations of $CaCl_2$ (0−10 mM). Assays were preincubated for 10 min at 37 °C, and the reaction was initiated by the addition of PAD4 (0.2 μM final). After 20 min, the reaction was quenched, and the amount of Cit produced was quantified using the methodology outlined above for the kinetic assay. In all cases, product formation did not exceed 10% turnover. Data were plotted to eq 3, using the Kaleidagraph version 3.09 software package.

$$v/V_{max} = [Ca^{2+}]^n/(K_d + [Ca^{2+}]^n) \quad (3)$$

The pH dependence of calcium activation was evaluated between pH 6.0 and pH 8.5 using a multicomponent buffering system containing 50 mM Tris-HCl/50 mM Bis-Tris/100 mM sodium acetate, 50 mM NaCl, 2 mM DTT, and 10 mM BAEE. Assays were preincubated for 10 min at 37 °C, at which point PAD4 (0.2 μM final concentration) was added to initiate the reaction. Data were fit to eq 3, using the Kaleidagraph version 3.09 software package.

Partial Proteolysis Experiments. Purified GST-cleaved PAD4 (~1 μg) was incubated in the absence or presence of subtilisin (3.3 μg/mL final concentration) for partial proteolysis reactions. These reactions were allowed to proceed for 90 min on ice. Reactions were quenched by the addition of phenylmethanesulfonyl fluoride to a final concentration of 5 mM. The proteolytic fragments generated by this procedure were then separated by 15% SDS−polyacrylamide gel electrophoresis. Reaction buffers consisted of a solution of 100 mM Tris-HCl, pH 7.6, 50 mM NaCl, and 5 mM DTT in a final volume of 20 μL. Barium, calcium, magnesium, manganese, samarium, strontium, zinc, and BAEE were used for substrate and metal ion protection studies at a final concentration of 10 mM. Control reactions, using BSA in place of PAD4, revealed that none of the metal ions used for the protection studies inhibited the activity of subtilisin.

*Synthesis of N-α-Benzoyl-N^G-monomethylarginine (**5a**).* A solution of 0.02 mL (0.15 mmol) of benzoyl chloride in 5 mL of methylene chloride was added to a solution of 25 mg (0.13 mmol) of N^G-monomethylarginine in 10 mL of ddH_2O containing 500 mg (6 mmol) of sodium bicarbonate. The

mixture was stirred vigorously for 16 h at room temperature. The reaction mixture was then acidified, and the organics were removed under vacuum. The remaining solution was applied to a preparative C18 reverse-phase column, and *N*-α-benzoyl-N^G-monomethylarginine was purified by high-performance liquid chromatography, using a linear H_2O/acetonitrile/0.1% trifluoroacetic acid gradient. A white solid was obtained (82.3% yield). ESIHRMS ($M + H^+$) calcd for $C_{14}H_{20}N_4O_3$ 293.1613, found 293.1621. ^{1}H NMR (400 MHz, DMSO-d_6) δ 8.66 (d, 1H), 7.90 (d, 2H), 7.58−7.46 (m, 5H), 7.41 (m, 1H), 7.34 (m, 1H), 4.41 (m, 1H), 3.17 (m, 2H), 2.73 (d, 3H), 1.88 (m, 2H), 1.59 (m, 2H). ^{13}C NMR (400 MHz, DMSO-d_6) δ 173.5, 166.5, 156.2, 133.8, 131.3, 128.2, 127.4, 52.1, 48.5, 27.8, 27.6, 25.4.

*Synthesis of N-α-Benzoyl(asymmetric)-N^G,N^G-dimethylarginine (**6a**).* The above procedure was carried out using 25 mg (0.09 mmol) of N^G,N^G-dimethylarginine. A white solid was obtained in 78.2% yield. ESIHRMS ($M + H^+$) calcd for $C_{15}H_{22}N_4O_3$ 307.1770, found 307.1776. ^{1}H NMR (400 MHz, DMSO-d_6) δ 8.66 (d, 1H), 7.90 (d, 2H), 7.58−7.47 (m, 5H), 7.37 (m, 1H), 4.43 (m, 1H), 3.19 (m, 2H), 2.94 (s, 6H), 1.89 (m, 2H), 1.64 (m, 2H). ^{13}C NMR (400 MHz, DMSO-d_6) δ 173.5, 166.5, 155.6, 133.8, 131.4, 128.2, 127.3, 52.1, 41.3, 38.0, 27.7, 25.4.

*Synthesis of N-α-Benzoyl(symmetric)-N^G,$N^{G\prime}$-dimethylarginine (**7a**).* The above procedure was carried out using 25 mg (0.09 mmol) of N^G,$N^{G\prime}$-dimethylarginine. A white solid was obtained in 83.7% yield. ESIHRMS ($M + H^+$) calcd for $C_{15}H_{22}N_4O_3$ 307.1770, found 307.1772. ^{1}H NMR (400 MHz, DMSO-d_6) δ 8.67 (d, 1H), 7.90 (d, 2H), 7.57−7.48 (m, 5H), 7.41 (m, 1H), 4.42 (m, 1H), 3.16 (m, 2H), 2.74 (d, 6H), 1.89 (m, 2H), 1.62 (m, 2H). ^{13}C NMR (400 MHz, DMSO-d_6) δ 174.0, 167.0, 155.7, 134.3, 131.8, 128.7, 127.9, 52.6, 40.9, 28.4, 28.2, 25.8.

*Synthesis of N-α-Benzoyl- N^G-monomethylarginine Ethyl Ester (**5b**).* Fischer esterification was carried out on *N*-α-benzoyl-N^G-monomethylarginine. *N*-α-Benzoyl-N^G-monomethylarginine (25 mg, 0.08 mmol) was dissolved in 10 mL of ethanol. Three drops of concentrated sulfuric acid were added to the reaction mixture which was then refluxed for 3 h. The reaction mixture was cooled and applied to a preparative C18 reverse-phase column. *N*-α-Benzoyl-N^G-monomethylarginine ethyl ester was purified by high-performance liquid chromatography using a linear H_2O/acetonitrile/0.05% trifluoroacetic acid gradient. A white solid was obtained in 87.5% yield. ESIHRMS ($M + H^+$) calcd for $C_{15}H_{22}N_4O_3$ 321.1912, found 321.1926. ^{1}H NMR (300 MHz, DMSO-d_6) δ 8.74 (d, 1H), 7.86 (d, 2H), 7.56−7.44 (m, 5H), 7.39 (m, 1H), 7.31 (m, 1H), 4.42 (m, 1H), 4.08 (q, 2H), 3.14 (m, 2H), 2.71 (d, 3H), 1.79 (m, 2H), 1.55 (m, 2H), 1.17 (t, 3H). ^{13}C NMR (400 MHz, DMSO-d_6) δ 171.9, 166.6, 156.1, 133.7, 131.5, 128.2, 127.4, 60.5, 52.3, 48.5, 27.8, 27.5, 25.3, 14.0.

*Synthesis of N-α-Benzoyl-N^G,N^G(asymmetric)-dimethylarginine Ethyl Ester (**6b**).* Fischer esterification was carried out as described above using 22 mg (0.07 mmol) of *N*-α-benzoyl-N^G,N^G(asymmetric)-dimethylarginine. A white solid was obtained in 86% yield. ESIHRMS ($M + H^+$) calcd for $C_{17}H_{27}N_4O_3$ 335.2083, found 335.2079. ^{1}H NMR (400 MHz, DMSO-d_6) δ 8.76 (d, 1H), 7.87 (d, 2H), 7.57−7.49 (m, 5H), 7.41 (m, 1H), 4.46 (m, 1H), 4.13 (q, 2H), 3.19 (m, 2H), 2.94 (s, 6H), 1.87 (m, 2H), 1.62 (m, 2H), 1.20 (t, 3H).^{13}C NMR (400 MHz, DMSO-d_6) δ 172.0, 166.6, 155.6, 133.7, 131.4, 128.2, 127.4, 60.5, 52.2, 41.2, 38.0, 27.5, 25.2, 14.0.

*Synthesis of N-α-Benzoyl-N^G,$N^{G\prime}$(symmetric)-dimethylarginine Ethyl Ester (**7b**).* Fischer esterification was carried out as described above using 23 mg (0.08 mmol) of *N*-α-benzoyl-N^G,$N^{G\prime}$(symmetric)-dimethylarginine. A white solid was obtained in 99% yield. ESIHRMS ($M + H^+$) calcd for $C_{17}H_{27}N_4O_3$ 335.2083, found 335.2084. ^{1}H NMR (300 MHz, DMSO-d_6) δ 8.75 (d, 1H), 7.87 (d, 2H), 7.55−7.42 (m, 5H), 7.37 (m, 1H), 4.41 (m, 1H), 4.13 (q, 2H), 3.12 (m, 2H), 2.72 (d, 6H), 1.80 (m, 2H), 1.58 (m, 2H), 1.20 (t, 3H). ^{13}C NMR (300 MHz, DMSO-d_6) δ 172.8, 167.4, 155.9, 134.4, 132.2, 129.0, 128.1, 61.2, 53.0, 41.1, 28.7, 28.6, 25.9, 14.8.

Kinetic Analysis of N-α-Benzoylated Methylarginine Derivatives. Variable concentrations of *N*-α-benzoylated methylarginine derivatives were assayed in duplicate using the methodology described above for the kinetic assay. When possible, experimentally determined initial rates were plotted to the equation

$$v = V_{max}/K_m[S] \quad (4)$$

using the Kaleidagraph version 3.09 software package. Correlation coefficients for the linear fits were typically greater than 0.99. On the basis of the assumptions that the ethyl esters were completely racemized during esterification and that the *R* enantiomers are neither substrates nor inhibitors of the enzyme, the concentrations of these compounds were halved for the calculation of *V*/*K*.

Peptide Synthesis. Peptides were synthesized on the automated peptide synthesizer, PS3 (Protein Technologies). Upon completion of synthesis, the resin was washed three times each with dimethylformamide (DMF), ethanol, and methylene chloride. Cleavage was accomplished by rotation of the resin with 20 mL of reagent K [trifluoroacetic acid:phenol:H_2O:thioanisole:ethanedithiol (35:2:2:2:1)] for 2 h at room temperature, at which point peptides were precipitated with ice-cold diethyl ether. The precipitate was isolated by centrifugation (3000*g*, 10 min) and washed twice with ice-cold diethyl ether. The product was then flash frozen and lyophilized. The lyophilized powder was resuspended in H_2O and purified by high-performance liquid chromatography using ddH_2O/acetonitrile/0.05% TFA as the mobile phase. The structures of the peptides synthesized for these studies were confirmed by electrospray mass spectrometry: ESIMS ($M + H^+$) calcd for H4−13 1141.3, found 1142; ESIMS ($M + H^+$) calcd for H4−15 1286.4, found 1287; ESIMS ($M + H^+$) calcd for H4−15 R3MMA 1300.4, found 1301; ESIMS ($M + H^+$) calcd for H4−15 R3ADMA 1314.4, found 1315; ESIMS ($M + H^+$) calcd for H4−21 2090.4, found 2091; ESIMS ($M + H^+$) calcd for H4−21 R3K 2062.4, found 2063.

RESULTS

Protein Expression and Purification. PAD4 was expressed as a GST fusion protein and purified analogously to published methods (*30*). The GST tag was removed with PreScission protease, thereby affording the purification of the GST-cleaved form of the enzyme in modest yield (∼0.25 mg/L of *E. coli* cell culture) but high purity. MALDI mass spectra of purified GST-cleaved PAD4 revealed a minimal (0.3%) difference between the expected and observed masses [*m*/*z*

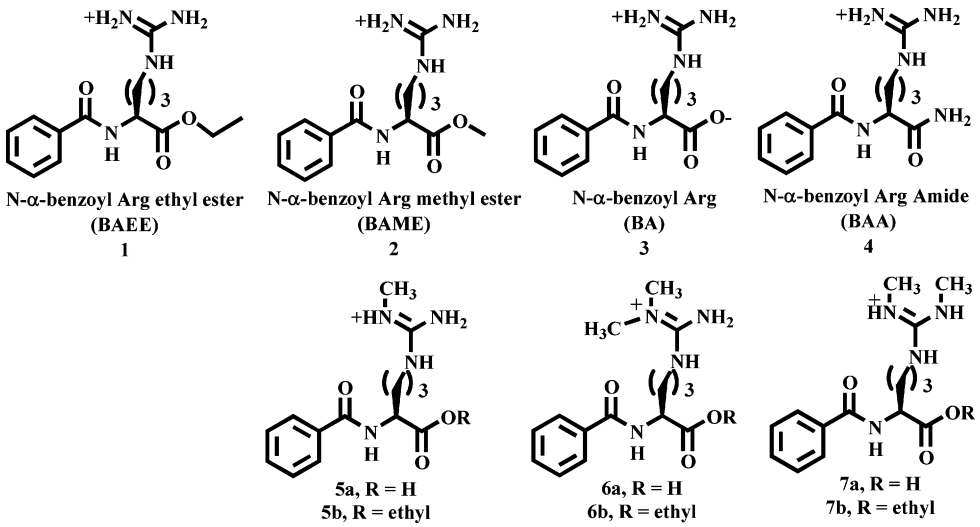

FIGURE 2: Structures of N-α-benzoylated arginines used in these studies.

Table 1: PAD4 Catalyzes the Hydrolytic Deimination of BAEE[a]

	predicted $[M + Na^+]^+$		
reaction type	$H_2{}^{16}O$	$H_2{}^{18}O$	obsd $[M + Na^+]^+$
hydrolytic	330	332	332
oxidative	330	330	

[a] Recombinant human PAD4 was used to catalyze in vitro deimination reactions in either normal or ^{18}O-labeled water. BAEE was used as the substrate.

74879, 74639 (exp, obsd)]. This is consistent with the purification of intact full-length PAD4, although it should be noted that the slight mass difference could represent the loss of one to two amino acids after the removal of the GST tag.

PAD4 Is a Hydrolase. Hydrolytic and oxidative mechanisms of deimination were differentiated by performing large-scale PAD4-catalyzed deimination reactions in either normal or ^{18}O-labeled water, because a 2 unit difference will be apparent in mass spectra if water is the source of molecular oxygen. Deimination reactions, using BAEE as the substrate (Figure 2), were incubated for 3 h at 37 °C; at this point, the deiminated product was isolated by reverse-phase chromatography and analyzed by mass spectrometry. For the PAD4-catalyzed reaction, a 2 unit mass difference was observed (Table 1). These studies therefore establish that the source of molecular oxygen in the product is H_2O, demonstrating that PAD4 catalyzes the hydrolytic deimination of Arg residues in proteins.

PAD4 Catalyzes the Production of Ammonia. On the basis of the structure of PAD4 and mechanistic data from related systems (*28*, *33*−*35*), we favor a mechanism in which a low pK_a active site Cys (Cys645) acts as a nucleophile to generate a tetrahedral adduct, which collapses to form a stable amidino-Cys intermediate and ammonia. Hydrolysis of the intermediate leads to the formation of Cit (Figure 3). Because the first tetrathedral intermediate in the PAD4-catalyzed reaction could also collapse to form ornithine, as is the case in the reaction catalyzed by amidinotransferase [a PAD4 structural homologue (*36*)], the ability of PAD4 to catalyze the formation of ammonia, and not ornithine, was examined using a previously described fluorometric assay (*32*). For these studies, the amounts of both ammonia and ureido-containing compounds produced during time course experiments were quantified in parallel. The results of these studies (Figure 4) indicate that ammonia and the ureido-containing compound are produced in equimolar amounts, thereby confirming that PAD4 catalyzes the hydrolytic deimination of Arg residues to produce ammonia and Cit.

Metal Dependence of PAD4. While calcium is a known regulator of PAD4 activity, the general metal dependence of this enzyme is poorly characterized. Therefore, the ability of several cations to enhance PAD4 activity was evaluated. These metal ions included barium, calcium, magnesium, manganese, samarium, strontium, and zinc. Barium, magnesium, and strontium were tested because they, like calcium, are group 2 metals. Manganese and zinc were tested because they are physiologically relevant divalent cations. Samarium was tested because it is often used as a replacement for calcium in crystallographic studies (*37*−*39*). For these experiments the amount of Cit formation was monitored. Care was taken to ensure that none of the metal ions tested interfered with the assay. Using this assay, the activity associated with these metal ions was minimal (≤2.5% of control) when compared to the levels of activation afforded by calcium (Table 2). Thus, PAD4 activity is highly calcium specific.

Calcium Dependence of PAD4. To further characterize the calcium dependence of PAD4, the concentration dependence of PAD4 activation by this metal ion was determined for a number of benzoylated Arg derivatives (Table 3). The calcium dependence of PAD4 with BAEE, a representative example, is depicted in Figure 5. The data were fit to a sigmoidal curve, indicating positive cooperativity, and the concentrations of calcium that yield half-maximal activity ($K_{0.5}$) are in the mid to high micromolar range. The fact that the Hill coefficients range from 1.5 to 3.0 indicates that multiple calcium ions are required for PAD4 activation, consistent with structural studies on PAD4 (*28*).

Partial Proteolysis Studies on PAD4. Because calcium could regulate PAD4 activity by triggering a conformational change, partial proteolysis was used to probe for the existence of a calcium-induced conformational change. Incubation of PAD4 with limiting amounts of subtilisin, in the absence of calcium, results in the formation of one major and two minor fragments with apparent molecular masses of 63.5, 36.0, and

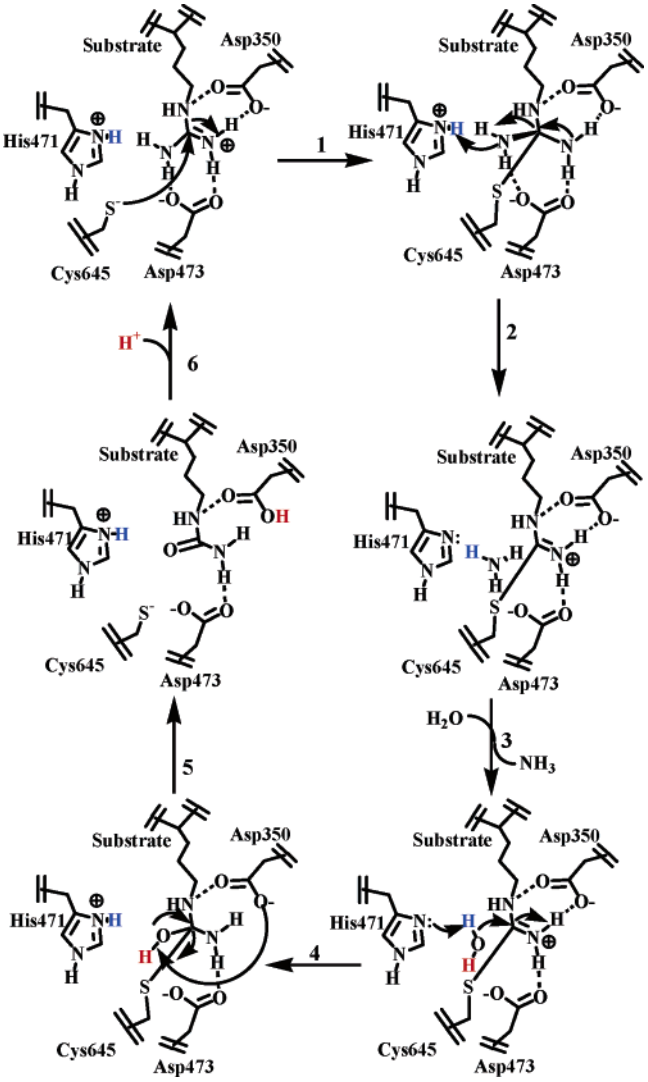

FIGURE 3: Proposed PAD4 catalytic mechanism. A low pK_a active site Cys is the nucleophile in this reaction, leading to the formation of an amidino-Cys intermediate (steps 1 and 2). While His471 is drawn as the general base, a plausible alternative mechanism involves product-assisted catalysis i.e., deprotonation of a water molecule by ammonia (steps 3 and 4). Asp350 is appropriately positioned to accept a proton from the tetrahedral intermediate and thereby promote the anti elimination of the Cys nucleophile (step 5). Asp350 could donate this proton to bulk solvent to regenerate the initial form of the enzyme (step 6).

21.5 kDa; whereas in the presence of calcium, and to a lesser extent BAEE, partial proteolysis of PAD4 is inhibited (Figure 6). These results are consistent with calcium binding causing a conformational change. To identify the specific domains encompassing these fragments, we have attempted N-terminal sequencing of the bands observed on SDS−PAGE gels. Unfortunately, interpretable N-terminal sequencing data have not been forthcoming. While this difficulty is likely due to the relatively nonspecific sequence specificity of subtilisin, it is further complicated by our inability to purify PAD4 in sufficient quantities to ease these, and related, analyses. Partial proteolysis with other more specific proteases (e.g., V8 protease and trypsin) has been attempted, but we have been unable to detect a calcium-dependent conformational change with these proteases.

Metal Inhibition of PAD4. To further examine the metal dependence of PAD4 activity, the ability of specific cations

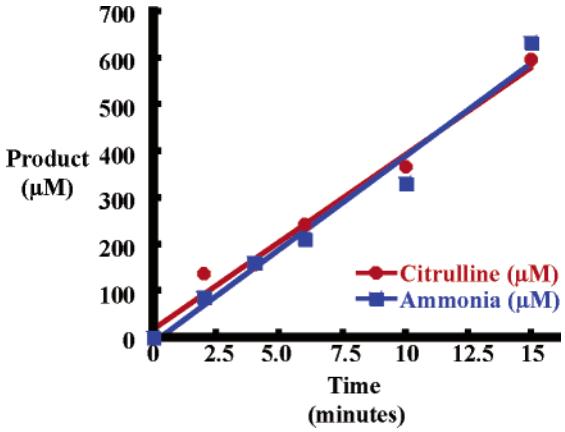

FIGURE 4: PAD4 catalyzes the formation of Cit and ammonia in equimolar amounts. Time course experiments were performed in parallel at 37 °C, and the amounts of Cit and ammonia produced were quantified (see Materials and Methods for experimental details).

Table 2: Metal Dependence of PAD4[a]

metal	% activity[b]	IC_{50} (mM)[c]	partial proteolysis[d]
calcium	100	NI	P
barium	≤2.5	4.0	NP
magnesium	<1.0	10.0	NP
manganese	≤1.3	0.75	P
samarium	≤2.2	0.04	P
strontium	≤2.0	10.0	NP
zinc	≤2.0	0.75	P

[a] PAD4 is a Ca^{2+}-specific enzyme. Samarium sulfate and the chloride salts of calcium, barium, magnesium, manganese, strontium, and zinc were used for these studies. [b] Metal dependence assays were performed in the presence of the indicated metal ions (10 mM final). [c] IC_{50}s were determined using variable concentrations of the indicated metal ions and a fixed concentration of calcium (1 mM final; NI = no inhibition). [d] The results of the partial proteolysis studies are summarized (P = protection, NP = no protection).

Table 3: PAD4 Calcium Dependence for Benzoylated Arg Substrates[a]

substrate	$K_{0.5}$ (μM)[b]	n[c]
BAEE	560 ± 40	3.0 ± 0.1
BAME	670 ± 120	2.0 ± 0.3
BA	260 ± 40	1.5 ± 0.1
BAA	130 ± 100	2.2 ± 0.4

[a] Activity assays were performed in duplicate at 37 °C, and these generally agreed within 20%. [b] $K_{0.5}$ is the concentration of calcium that yields half-maximal activity. $K_{0.5}$ is equal to the $n(K_d)^{1/2}$. [c] n is the Hill coefficient.

to inhibit PAD4 activity was evaluated. For these studies 1 mM $CaCl_2$ was used to activate PAD4 in the presence of various concentrations of the indicated metal ions, and IC_{50}s were determined (Table 2). Manganese, samarium, and zinc strongly inhibited the calcium-induced activation of PAD4, whereas smaller levels of inhibition were observed for barium, magnesium, and strontium. The results of these metal inhibition studies are generally consistent with observations obtained for a PAD isozyme purified from rat epidermis (*23*).

While the reasons for these effects were unclear, it seemed likely that one or more of the inhibitory metal ions exerted their effect by preventing the calcium-induced conformational change that is required for PAD4 activation or, alternatively, permit a conformational change but do not allow PAD4 to

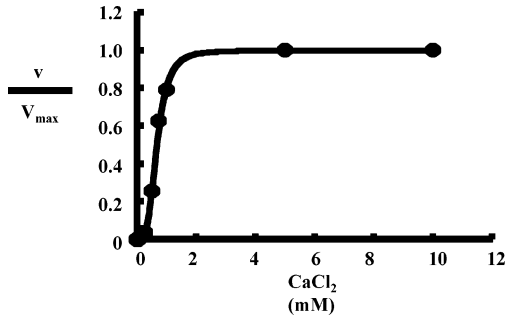

FIGURE 5: Calcium dependence of PAD4. Activity assays were performed in duplicate with saturating amounts of BAEE and the data fit to $v/V_{max} = ([Ca^{2+}]^n)/(K_d + [Ca^{2+}]^n)$.

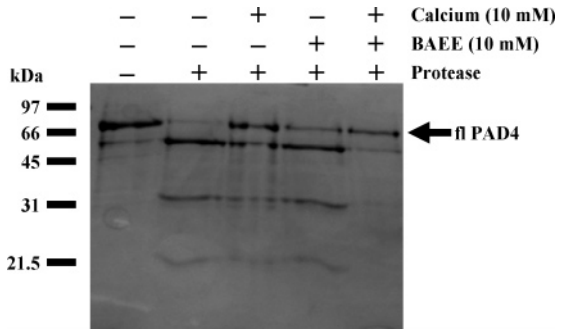

FIGURE 6: Partial proteolysis of full-length (fl) PAD4. Subtilisin (0.33 μg/mL) was incubated with ~1 μg of PAD4 for 90 min on ice in the absence or presence of the indicated components. Reactions were separated by 15% SDS−PAGE and proteins visualized with Coomassie Brilliant Blue.

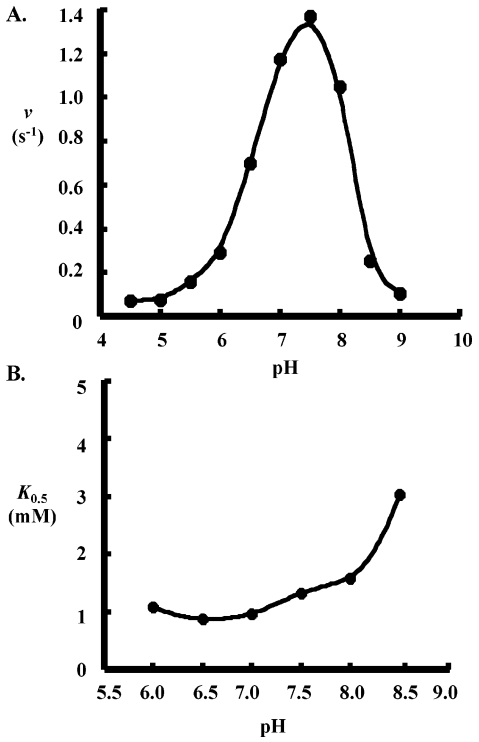

FIGURE 7: pH dependence of PAD4 activity and calcium activation. (A) The pH dependence of PAD4 activity was evaluated using a multicomponent buffering system (see Materials and Methods for experimental details). Activity assays were performed in duplicate using a fixed concentration of BAEE as the substrate (1 mM BAEE, $0.74K_m$). pK_a values were estimated by fitting the data to $\log(k_{cat}/K_m)_{app} = \log[k_{cat}/K_m(1 + H/K_1 + K_2/H)]$. (B) The pH dependence of calcium activation was determined by measuring the concentration of calcium required to activate PAD4 between pH 6.0 and pH 8.5, analogously to the methods described in Figure 5, except that the multicomponent buffering system was used for these studies. Experimentally derived values for $K_{0.5}$ are plotted against pH. While Hill coefficients were comparable to those obtained for BAEE and other PAD4 substrates, they were somewhat variable, ranging from 2.3 to 3.6, but showed no obvious trend with changes in pH.

adopt a conformation that is catalytically competent. These possibilities were investigated by partial proteolysis studies (Table 2), and it was determined that only manganese, samarium, and zinc, three of the strongest inhibitors of calcium activation, prevent the partial proteolysis of PAD4 to an extent that is similar to the level afforded by calcium. None of the metal ions utilized in these studies could inhibit the subtilisin-catalyzed proteolysis of BSA (data not shown), thereby indicating that these metal ions cause PAD4 to adopt a conformation that is not catalytically competent.

pH Optimum of PAD4 Activity. To identify the pH optimum, the pH dependence of PAD4 activity was evaluated over a broad pH range (pH 4.5−9.0), using BAEE at a fixed concentration of 1 mM ($0.74K_m$). These studies indicate that the pH rate profiles are bell shaped and, assuming a model with two ionizable groups, suggest the existence of two catalytically important residues with pK_a values of ~6.2 and ~7.9 (Figure 7A). The pH optimum was pH 7.6. Cit production at each of the pH values was linear with time, indicating that the pH-dependent decrease in activity is due to changes in the protonation state of the enzyme and not due to denaturation of the enzyme. Because optimum activity was observed at pH 7.6, further kinetic studies were carried out at this pH.

The pH dependence of calcium activation was evaluated between pH 6.0 and pH 8.5, using a multicomponent buffering system. This pH range was chosen because the greatest change in PAD4 activity is observed between these pH values. The results obtained indicate that the calcium dependence of PAD4 is essentially pH-independent over this range (the change in $K_{0.5}$ is less than 3-fold), which is consistent with the fact that the residues lining the known metal binding sites (i.e., Asp, Asn, and Glu) do not possess side chains that typically ionize between pH 6.0 and pH 8.5. The small change in $K_{0.5}$, which correlated with increasing basicity, could be due to the greater difficulty in desolvating calcium hydroxide species at higher pH values.

Kinetic Characterization of PAD4 Activity. The steady-state kinetic parameters of the enzyme were determined for BAEE, BAME, BAA, and BA (Figure 2, Table 4) using a discontinuous assay that monitors ureido group formation. Activity assays, which were linear with respect to time and enzyme concentration, were performed in duplicate and the values typically agreed within 20%. K_m values for benzoylated Arg derivatives range from 0.25 to 1.66 mM with k_{cat} values ranging from ~2.8 to 5.9 s^{-1}. These values are in reasonable agreement with values previously obtained for recombinant PAD4 (*22*, *29*) and nonhuman PAD activities purified from a variety of tissue sources including rat epidermis, bovine brain, rabbit skeletal muscle, and guinea pig hair follicles (*23*−*27*). Kinetic parameters for either Arg or Arg ethyl ester could not be accurately determined with PAD4 because these compounds are such poor substrates ($V/K \leq 2$ M^{-1} s^{-1}), thereby indicating that N-acylation is absolutely required for the productive recognition of substrates by PAD4.

Table 4: PAD4 Steady-State Kinetic Parameters for Benzoylated Arg Substrates[a]

substrate	K_m (mM)	k_{cat} (s^{-1})	k_{cat}/K_m ($s^{-1}\,M^{-1}$)
BAEE	1.36 ± 0.19	5.94 ± 0.26	4400
BAME	1.66 ± 0.26	5.57 ± 0.28	3300
BA	0.41 ± 0.04	3.35 ± 0.12	8100
BAA	0.25 ± 0.06	2.76 ± 0.16	11000
Arg	ND[b]	ND	<0.01
Arg ethyl ester	ND	ND	<2.0
5a	ND	ND	<1.8[c]
5b	ND	ND	<31.3[c]
6a	ND	ND	<3.6[c]
6b	ND	ND	<9.0[c]
7a	ND	ND	<0.4[c]
7b	ND	ND	<4.6[c]

[a] Kinetic parameters were determined in duplicate at 37 °C. PAD4 activity was linear with time and enzyme concentration in the range employed. [b] ND = not determined. [c] The *V/K* for these compounds was determined using the equation $v = k_{cat}/K_m([E_t][S])$, when possible.

Kinetic Characterization of Peptide Substrates. A series of peptides, based on the N-terminus of histone H4, were synthesized by standard Fmoc-based solid-phase peptide synthesis and purified by preparative HPLC. Histone H4 peptides were chosen for these studies because (1) the majority of known histone modifications occur in the N-terminal tails of histone proteins (*40*−*42*), (2) peptides based on histone N-termini are often used for such kinetic analyses (*43*−*45*), and (3) Arg3 in histone H4 is known to be modified by PAD4 in vivo (*20*, *46*).

The steady-state kinetic parameters for these peptides were determined using the methodology described above for the kinetic characterization of the benzoylated arginine derivatives. The results of these experiments (Table 5) revealed that the kinetic values for peptide substrates are comparable to those obtained for BAEE (the *V/K* for the H4−21 peptide is only 2.2-fold higher than the *V/K* for BAEE), suggesting that benzoylated Arg residues are good models for characterizing PAD4 activity.

The observation that the H4−13 peptide, whose sequence consists of a free amino group α to Arg3, is such a poor PAD4 substrate ($V/K < 27.0\ M^{-1}\ s^{-1}$) is consistent with the fact that free L-Arg and Arg ethyl ester are very poor PAD4 substrates. These results thereby confirm that a minimum of one additional amino acid N-terminal to the site of deimination is absolutely required for productive deimination of substrates by PAD4.

The fact that the H4−15 peptide, which contains only a single Arg residue, is a PAD4 substrate indicates that H4 Arg3 is deiminated in vitro, consistent with this residue being a major site of deimination in vivo (*20*, *46*). The 23-fold decrease in the *V/K* for the H4−21 R3K peptide, relative to the *V/K* for the H4−21 peptide, is also consistent with H4 Arg3 being a major site of deimination by PAD4. While the kinetic values obtained for the H4−21 R3K peptide also suggest that H4 Arg17 and H4 Arg19 are deiminated in vitro, the significant decrease in the *V/K* for this peptide indicates that PAD4 can modify Arg residues regioselectively within the context of a peptide substrate.

Methylated Arg Residues Are Poor PAD4 Substrates. It has been suggested that PAD4 possesses the ability to catalyze the deimination of posttranslationally methylated Arg residues as a mechanism to reverse the physiological effects of Arg methylation (*47*). While such an activity was recently noted for PAD4 (*20*, *21*), the rate at which this reaction is catalyzed has not been quantified.

Therefore, benzoylated methyl-Arg derivatives were synthesized to quantitatively examine the rate at which PAD4 catalyzes their deimination. These compounds were synthesized under Schotten−Baumann conditions (*48*), as outlined in Scheme 1, using near stoichiometric amounts of benzoyl chloride to minimize side reactions with the guanidinium group. The synthesis and purification of these Arg derivatives and their ethyl esters were facile and occurred in good yield (typically >75%), and the structures were confirmed by NMR and mass spectrometry.

The ability of PAD4 to catalyze the deimination of compounds **5a**, **6a**, and **7a** was evaluated, and the results indicate that the *V/K*s for these compounds are 4.5×10^3-fold to 2.0×10^4-fold worse than the *V/K* for benzoyl-Arg (BA), the unmethylated analogue (Table 4). The ethyl esters of these compounds (**5b**, **6b**, and **7b**) were also evaluated; and while the rates at which they are deiminated are improved (∼5- to 30-fold relative to **5a**, **6a**, and **7a**), they are still poor substrates: the *V/K*s are decreased 150−1000-fold relative to BAEE, the unmethylated analogue. These data could suggest that methylated Arg residues are not physiologically relevant substrates of PAD4.

To further examine the ability of this enzyme to catalyze the deimination of methylated substrates, peptides that incorporate either monomethylated (MMA) (H4−15 R3MMA) or asymmetrically dimethylated Arg (ADMA) (H4−15 R3ADMA) at a single position were synthesized. The sequence of these peptides was chosen because the H4−15 peptide is a good PAD4 substrate that contains only a single Arg residue that is known to be deiminated both in vitro and in vivo. Monomethylated and asymmetrically dimethylated Arg were incorporated at H4 Arg3 because protein arginine methyltransferase 1 (PRMT1) asymmetrically dimethylates this residue in vitro (*49*) and this residue is known to be monomethylated in vivo (*50*). The ability of PAD4 to catalyze the deimination of the H4−15 R3MMA and H4−15 R3ADMA peptides was evaluated, and the results indicate that the *V/K*s for these peptides are decreased by at least 585-fold, relative to the *V/K* for the H4−15 peptide (Table 5). Thus, methylated Arg residues are quite poor substrates for full-length PAD4 in vitro, regardless of whether this residue is in the context of a small molecule or a peptide substrate.

DISCUSSION

While the contribution of PAD activity, and PAD4 in particular, to the onset and progression of RA is currently unclear, the preponderance of genetic, biochemical, and serological evidence indicates that there is a link between a dysregulated PAD activity and this debilitating autoimmune disorder, thereby illustrating the importance of characterizing the in vivo role of PAD activity. One approach to studying the in vivo role of an enzyme is the development of specific molecular probes that prevent catalysis. Therefore, studies of PAD4 catalysis were initiated to identify important mechanistic features that could be exploited for the design and synthesis of potent and selective PAD4 inhibitors, in this way aiding our ultimate goal of developing such compounds.

Table 5: PAD4 Steady-State Kinetic Parameters for Peptide Substrates[a]

substrate	peptide sequence	K_m (mM)	k_{cat} (s^{-1})	k_{cat}/K_m (s^{-1} M^{-1})
H4−21	NH_3^+-S[1]G**R**GKGGKGLGKGGAK**R**H**R**KV[21]-COO^-	0.67 ± 0.03	6.55 ± 0.10	9700
H4−21 R3K	NH_3^+-S[1]G**K**GKGGKGLGKGGAK**R**H**R**KV[21]-COO^-	1.23 ± 0.06	2.94 ± 0.20	420
H4−15	NH_3^+-S[1]G**R**GKGGKGLGKGGA[15]-COO^-	2.68 ± 0.16	3.13 ± 0.36	1170
H4−15 R3MMA	NH_3^+-S[1]G**X**GKGGKGLGKGGA[15]-COO^- X = MMA[d]	ND[b]	ND	≤30.0[c]
H4−15 R3ADMA	NH_3^+-S[1]G**X**GKGGKGLGKGGA[15]-COO^- X = ADMA[e]	ND	ND	≤2.0[c]
H4−13	NH_3^+-**R**[3]GKGGKGLGKGGA[15]-COO^-	ND	ND	≤27.0[c]

[a] Kinetic parameters were determined in duplicate at 37 °C. PAD4 activity was linear with time and enzyme concentration in the range employed. [b] ND = not determined. [c] The *V/K* for these compounds was determined using the equation $v = k_{cat}/K_m([E_t][S])$, when possible. [d] MMA = monomethyl-Arg. [e] ADMA = asymmetric dimethyl-Arg.

Scheme 1: Synthesis of Asymmetric Dimethylbenzoyl-L-arginine Ethyl Ester (**6b**)

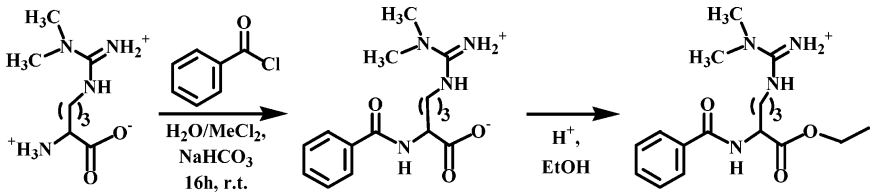

PAD4 Reaction Mechanism. On the basis of historical precedent, it was expected that PAD4 would catalyze the hydrolytic deimination of Arg residues to produce ammonia and Cit. Nevertheless, experiments to establish the reaction catalyzed by this enzyme were undertaken because the substrates and products of this enzyme have not been fully established. This was an important line of investigation because a number of Arg-modifying enzymes (e.g., arginase, arginine deiminase, nitric oxide synthase, and amidinotransferase) catalyze reactions at the side chain guanidinium, generating a variety of products, including Cit, ornithine, ammonia, nitric oxide, and urea.

Initial studies focused on identifying the source of molecular oxygen (i.e., H_2O or O_2). Hydrolytic and oxidative deimination reactions were distinguished by performing large-scale deimination reactions in normal and ^{18}O-labeled water and then analyzing the products of the reaction by electrospray mass spectrometry. The results of these experiments clearly indicate that ^{18}O from water is incorporated into the product of the reaction. Our results are consistent with a recent proteomic study (*51*) that used ^{18}O from solvent to identify the PAD4-catalyzed sights of deimination in human fibrinogen. Thus, PAD4 catalyzes the hydrolytic deimination of benzoylated Arg derivatives to produce ^{18}O-labeled Cit.

While peaks corresponding to benzoylated ornithine ethyl ester were not apparent in mass spectra of the reaction products, these experiments could not rule out the possibility that PAD4 catalyzes the formation of ornithine and urea in appreciable amounts. This is an important question because PAD4 belongs to a superfamily of Arg-modifying enzymes [e.g., amidinotransferase (AT), arginine deiminase (ADI), and dimethylamine dimethylarginine hydrolase (DDAH)] (*28*, *36*, *52*) that share a common amidino-Cys intermediate (Figure 3) that can break down to form either ammonia, methylamine, dimethylamine (and Cit), or ornithine (and urea). Moreover, these experiments were necessary because our assay for Cit production will also measure urea production. Therefore, the ability of PAD4 to catalyze the formation of ammonia was directly evaluated. The results of these experiments clearly indicate that ammonia and an ureido-containing compound (i.e., Cit) are produced in equimolar amounts. This result is consistent with previous studies using a PAD from rabbit skeletal muscle (*25*) and indicates that PAD4 also catalyzes the hydrolytic deimination of Arg residues to produce Cit and ammonia.

Calcium Dependence of PAD4. While the calcium dependence of PAD activity is well documented (*25*−*27*), the general metal dependence of PAD4 activity is poorly characterized; and it is unclear whether this dependence is exclusive to calcium, i.e., whether PAD4 activity is dependent on the charge, size, and/or ligand binding properties of a particular activating metal ion. Therefore, the ability of several metal ions to enhance PAD4 activity was evaluated. These metal ions included barium, calcium, manganese, magnesium, samarium, strontium, and zinc. While samarium was not expected to activate PAD4, this metal ion was examined because it is often used as a replacement for calcium in crystallographic studies (*37*−*39*) and it was felt that it might compete with and inhibit calcium binding. The fact that significant levels of activity were only observed in the presence of calcium indicates that the activation of PAD4 is highly dependent on, and highly specific for, calcium. The fact that manganese, samarium, and zinc strongly inhibited the calcium-induced activation of PAD4, whereas smaller levels of inhibition were observed for barium, magnesium and strontium, suggests that relatively smaller, softer ions are better inhibitors of PAD4 than larger, harder ions.

In an effort to further characterize the calcium dependence of PAD4, the concentration dependence of calcium activation was evaluated for a variety of benzoylated Arg derivatives. Interestingly, the $K_{0.5}$ values are substrate-dependent and significantly higher (approximately 5−10-fold) than values (∼50 μM) obtained for rabbit skeletal muscle PAD (*27*). The elevated $K_{0.5}$ values could either reflect intrinsic differences between rabbit skeletal muscle PAD and recombinant PAD4 or be due to the presence of contaminating PAD4 proteolytic fragments that possess significantly lower Ca^{2+} activation constants. We favor the latter possibility because PAD4 is susceptible to proteolysis in situ and the $K_{0.5}$ values for

partially proteolyzed PAD4 are similar to those reported for rabbit skeletal muscle PAD (data not shown). Thus we note that care must be taken in the preparation of PAD4 to minimize its proteolytic degradation.

While the exact number of calcium ions required for activation is unknown, the fact that the calcium activation curves are sigmoidal suggests that the number must be greater than or equal to the Hill coefficient. Since in our hands the Hill coefficient ranged from 1.5 to 3.0, the minimum number of calcium ions required for PAD4 activation is likely greater than 3. This conclusion is consistent with structural studies on PAD4, which revealed the presence of electron density for up to five metal ions in the PAD4·BAA·calcium complex. However, it should be noted that the relative importance of each of these putative metals ions, and their respective binding sites, to PAD4 activation is incompletely established.

Calcium Binding Induces a Conformational Change in PAD4. One possible mechanism of calcium activation is a metal-dependent conformational change that converts an enzyme from the inactive to active state. The existence of such a calcium-dependent conformational change was probed by partial proteolysis because such studies are often used to monitor substrate- or metal-induced conformational changes (*53*, *54*). Our studies revealed that calcium protects PAD4 from proteolysis, consistent with calcium binding causing a conformational change. Structural studies on the PAD4 apoenzyme and the PAD4·calcium complex have confirmed our results and have additionally demonstrated that this conformational change involves a reorientation of active site residues (e.g., Cys645 and Asp350) into positions that are competent for substrate binding and catalysis (*28*). It should be noted that the five sites of calcium binding are at sites that are distant from the active site, thereby indicating that calcium plays a regulatory, rather than catalytic, role.

Physiological Implications of the PAD4 Calcium Dependence. It is noteworthy that the concentrations of calcium required for maximum activity (Table 3) are not physiologically relevant. Intracellular concentrations of calcium typically increase from ~200 nM in resting cells to ~1 μM in activated cells (*55*). The fact that the calcium $K_{0.5}$ values are significantly higher than this threshold suggests the existence of alternative PAD4 activating mechanisms. At least two possibilities exist: (1) proteolytic processing of the enzyme results in its activation in vivo by altering the calcium $K_{0.5}$, or (2) interacting proteins modulate the calcium dependence of PAD4. We are currently pursuing studies to address each of these possibilities. While it is also possible that the calcium dependence is substrate-dependent, a phenomenon that we (Table 3) and others (*56*) have observed, and that with specific substrates the $K_{0.5}$ values become physiologically relevant, we regard this as an unlikely possibility because the calcium dependence of PAD activity has been evaluated with a number of small molecule, peptide, and protein substrates and, to date, none of these compounds display $K_{0.5}$ values that are physiologically relevant.

Implications of pH Studies on the Catalytic Mechanism of PAD4. As noted above, our pH studies suggest the existence of two catalytically important residues with pK_a values of ~6.2 and ~7.9. Time course experiments indicate that the pH-dependent decrease in activity is due to changes in the protonation state of the enzyme and not due to denaturation of the enzyme. Since the $K_{0.5}$ values are essentially pH-independent over this pH range, it seems likely that these pK_a values represent residues that play an intimate role in catalysis. On the basis of the structure of PAD4, the two pK_as likely reflect the protonation states of Cys645 (pK_a ~ 6.2) and His471 (pK_a ~ 7.9), suggesting that for optimal activity Cys645 is deprotonated and His471 is protonated in the free form of the enzyme; i.e., the Cys645 thiolate is the nucleophilic species in the first step of the reaction and His471 acts as a general acid, donating a proton to aid the formation of ammonia.

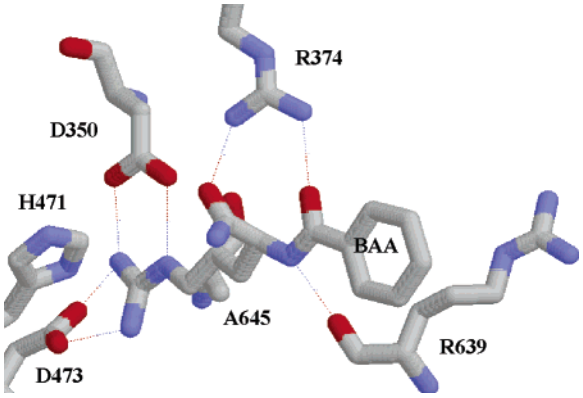

FIGURE 8: Active site of the PAD4·Ca^{2+}·BAA complex. Important active site residues, and the artificial substrate BAA, are highlighted in this figure. Dotted lines represent potential H-bonds between neighboring groups (distances are <3.0 Å in all cases). This figure was prepared with RasMol using the coordinates for the PAD4·Ca^{2+}·BAA complex (PDB ID: 1WDA).

While His471 is drawn as a general base in step 4, a plausible alternative mechanism involves product-assisted catalysis, i.e., deprotonation of a water molecule by ammonia to form the ammonium ion. Such a mechanism is consistent with the structure of PAD4 (*28*), which shows that a number of ordered water molecules are present in the direct vicinity of the departing molecule of ammonia. Further studies are being designed to validate the proposed mechanism of catalysis and thereby distinguish between general base- and product-assisted catalysis. These experiments are expected to yield interesting insights into the catalytic mechanism of PAD4 that will aid our design of PAD4 selective inhibitors.

Kinetic Characterization of PAD4 Activity. The steady-state kinetic parameters for a number of benzoylated Arg derivatives have been determined; while these substrates are not physiologically relevant, they have traditionally been used to study in vitro PAD activity (*23*−*27*). As discussed below, analyses with these compounds have provided useful insights into the substrate specificity requirements of PAD4. The current studies have revealed the critical requirement of N-terminal acylation for the productive recognition of substrates by PAD4: neither free Arg nor Arg ethyl ester are deiminated at appreciable rates (V/K < 2.0 M^{-1} s^{-1}).

On the basis of the structure of the PAD4·BAA·calcium complex (Figure 8), N-terminal acylation is likely required because (1) the guanidinium group of Arg374 is appropriately positioned to form an H-bond with the N-terminal main chain carbonyl of the substrate and (2) electrostatic repulsions between a positively charged N-terminal α-amino group and the guanidinium group of Arg374, which is 5 Å distant, would be expected to have a destabilizing effect on substrate binding.

In contrast, C-terminal acylation does not appear to be critical for substrate recognition, as evidenced by the fact that the *V/K*s for BA, BAEE, and BAA are quite similar. Electrostatic attractions between the α-carboxylate of BA and Arg374, which are less than 3 Å apart, likely explain why BA is such a good substrate.

Peptides based on the N-terminus of histone H4 were also synthesized, and their ability to act as PAD4 substrates was evaluated because such histone-based peptides are often used to characterize the substrate specificity of histone-modifying enzymes (*43*−*45*). The results of these experiments revealed that the kinetic parameters for histone-based peptide substrates are comparable to those obtained for the small molecule Arg derivatives examined in this study. Additionally, the results obtained for the H4−13 peptide indicate that N-terminal acylation is a critical requirement for substrate recognition, consistent with the results obtained for free L-Arg and Arg ethyl ester. The fact that the kinetic parameters for both small molecule and peptide substrates are comparable indicates that the benzoylated Arg derivatives are good models for studying the kinetics of the PAD4 reaction.

On the basis of the results of these kinetic studies, one would expect that PAD4 would be a nonspecific enzyme that could deiminate any Arg residue regardless of sequence context. However, this is not the case, as evidenced by the fact that the *V/K* for the H4−21 R3K peptide is decreased 23-fold, relative to the H4−21 peptide. This result is striking and indicates that PAD4 displays substrate selectivity. Consistent with this finding are recent reports indicating that PAD4 deiminates only a subset of the Arg residues in human fibrinogen in vitro and that Arg3 in both histone H2A and histone H4 is preferentially deiminated in vivo (*29*, *46*).

Since the second-order rate constants (*V/K*) observed for the deimination of peptide substrates are somewhat lower (<7-fold) than those obtained for other histone-modifying enzymes [e.g., the histone acetyltransferases p300 and PCAF (*45*, *57*)], it is possible that proteins are the preferred substrate for PAD4 and that long-range interactions, provided by sites far from the active site (>10 Å), are important for substrate recognition by this enzyme. A similar phenomenon has been observed for Cdc25, a protein phosphatase (*58*). While kinetic studies with human fibrinogen (*29*) suggest that this is not the case (the *V/K*s for small molecules, peptides, and fibrinogen are all in the 10^3-10^4 M^{-1} s^{-1} range), it should be noted that kinetic parameters derived in that study (*29*) are somewhat problematic because product formation exceeds substrate input. Thus further studies to address this issue are required.

PAD4 Poorly Catalyzes the Deimination of Methylated Arg Residues. Arg residues in a number of proteins are also subject to posttranslational methylation reactions, generating a variety of products, including monomethyl, asymmetric dimethyl, and symmetric dimethyl Arg residues. Because histones are subject to both Arg methylation and Arg deimination, it was suggested that PAD4 activity could represent a possible mechanism to reverse the physiological effects of Arg methylation (*47*). In fact, Kouzarides, Coonrod, Allis, and their co-workers have recently provided evidence that PAD4 can catalyze the deimination of monomethylated Arg residues in vivo (*20*, *21*); and while these studies elegantly suggest that PAD4 can catalyze the demethylimination of Arg residues, the rate of this reaction has not been quantified. Therefore, the ability of PAD4 to catalyze the deimination of methylated Arg residues was evaluated using N-α-benzoylated derivatives of monomethyl, asymmetric dimethyl, and symmetric dimethyl Arg.

Somewhat surprisingly, we observed that the second-order rate constants for the deimination of these compounds are 150-fold to 2.0×10^4-fold lower than the rate constants for the deimination of their unmethylated analogues. This was the case for both the free acids and the ethyl esters, as well as for peptide substrates containing either a single monomethyl or a single asymmetrically dimethylated Arg residue. Methylated Arg residues are likely poor substrates for full-length PAD4 because the active site is too small to readily accommodate the added bulk of the methyl groups.

Physiological Implications of the Slow Rate of Demethylimination. It is noteworthy that the in vitro rates of demethylimination are quite slow relative to the rate at which Arg residues are methylated. For example, the second-order rate constant for the methylation of histone H3 by CARM1/PRMT4 (*59*) is approximately 1000-fold faster than the highest rate of demethylimination observed in our laboratory. Thus, the ability of PAD4 to deiminate methylated Arg residues could be a promiscuous rather than physiologically relevant activity of PAD4.

However, immunofluoresence and chromatin immunoprecipitation data (*20*, *21*), while not definitive, do suggest that this reaction can occur in vivo, although we cannot rule out the possibility that the deimination of Arg residues precedes, and thereby antagonizes, the methylation of these residues, as suggested by Kouzarides (*21*). If PAD4 catalyzes the demethylimination reaction in vivo, there are at least three possibilities that could explain our inability to observe high rates of demethylimination in vitro. These possibilities include the following: (1) PAD4 can remove methyl groups from Arg residues only in the context of a protein substrate, (2) interacting proteins enhance the ability of PAD4 to catalyze this reaction in vivo, or (3) posttranslational modification (e.g., proteolytic processing) of the enzyme increases its ability to catalyze the demethylimination reaction. The first possibility seems unlikely because the rates of peptide and small molecule Arg deimination are quite similar and peptides are generally felt to be good mimics of histone N-termini. The latter two explanations are more plausible, and we are currently pursuing studies to address each of these possibilities.

Conclusions. In summary, an in vitro PAD4 assay has been used to characterize the reaction mechanism, metal dependence, calcium dependence, and substrate specificity of PAD4. Through these studies, we have established that PAD4 catalyzes the hydrolytic deimination of Arg residues to produce Cit and ammonia. Additionally, we have shown that calcium is the preferred activating metal ion and that metal binding to PAD4 causes a conformational change in the enzyme. These studies have also demonstrated that nonphysiological concentrations of calcium are required for enzyme activation, suggesting that additional layers of regulation must exist to activate this enzyme in vivo. Furthermore, the demonstration that methylated Arg residues are poor PAD4 substrates indicates that methylated Arg residues are unlikely to represent physiologically relevant substrates of the full-length enzyme in the absence of an as

yet unknown activating mechanism. Finally, the kinetic studies described herein will form the basis for the future design, synthesis, and evaluation of PAD4 selective inhibitors. It is expected that such inhibitors will be useful for deciphering the role of this enzyme in the various physiologically relevant processes in which its enzyme activity has been implicated (e.g., differentiation and transcriptional regulation).

ACKNOWLEDGMENT

The authors thank Michiyuki Yamada (Yokohama City University, Japan) for providing the PAD4 expression construct. The authors also thank Dr. Scott Goode and Chris Dockery (University of South Carolina) for help with the ICP-AES experiments. Mass spectra were recorded at the University of South Carolina Department of Chemistry and Biochemistry Mass Spectrometry Facility.

REFERENCES

1. Suzuki, A., Yamada, R., Chang, X., Tokuhiro, S., Sawada, T., Suzuki, M., Nagasaki, M., Nakayama-Hamada, M., Kawaida, R., Ono, M., Ohtsuki, M., Furukawa, H., Yoshino, S., Yukioka, M., Tohma, S., Matsubara, T., Wakitani, S., Teshima, R., Nishioka, Y., Sekine, A., Iida, A., Takahashi, A., Tsunoda, T., Nakamura, Y., and Yamamoto, K. (2003) Functional haplotypes of PADI4, encoding citrullinating enzyme peptidylarginine deiminase 4, are associated with rheumatoid arthritis, *Nat. Genet. 34*, 395−402.
2. Caponi, L., Petit-Teixeira, E., Sebbag, M., Bongiorni, F., Moscato, S., Pratesi, F., Pierlot, C., Osorio, J., Chapuy-Regaud, S., Guerrin, M., Cornelis, F., Serre, G., and Migliorini, P. (2004) A family-based study shows no association between rheumatoid arthritis and the PADI4 gene in a French caucasian population, *Ann. Rheum. Dis. 64*, 587−593.
3. Barton, A., Bowes, J., Eyre, S., Spreckley, K., Hinks, A., John, S., and Worthington, J. (2004) A functional haplotype of the PADI4 gene associated with rheumatoid arthritis in a Japanese population is not associated in a United Kingdom population, *Arthritis Rheum. 50*, 1117−1121.
4. Hoppe, B., Heymann, G. A., Tolou, F., Kiesewetter, H., Doerner, T., and Salama, A. (2004) High variability of peptidylarginine deiminase 4 (PADI4) in a healthy white population: characterization of six new variants of PADI4 exons 2−4 by a novel haplotype-specific sequencing-based approach, *J. Mol. Med. 82*, 762−767.
5. Vossenaar, E. R., Radstake, T. R., van der Heijden, A., van Mansum, M. A., Dieteren, C., de Rooij, D. J., Barrera, P., Zendman, A. J., and van Venrooij, W. J. (2004) Expression and activity of citrullinating peptidylarginine deiminase enzymes in monocytes and macrophages, *Ann. Rheum. Dis. 63*, 373−381.
6. Vossenaar, E. R., Despres, N., Lapointe, E., Van Der Heijden, A., Lora, M., Senshu, T., Van Venrooij, W. J., and Menard, H. A. (2004) Rheumatoid arthritis specific anti-Sa antibodies target citrullinated vimentin, *Arthritis Res. Ther. 6*, R142−R150.
7. Vossenaar, E. R., and Van Venrooij, W. J. (2004) Citrullinated proteins: sparks that may ignite the fire in rheumatoid arthritis, *Arthritis Res. Ther. 6*, 107−111.
8. Vossenaar, E. R., Zendman, A. J., van Venrooij, W. J., and Pruijn, G. J. (2003) PAD, a growing family of citrullinating enzymes: genes, features and involvement in disease, *BioEssays 25*, 1106−1118.
9. Schellekens, G. A., de Jong, B. A., van den Hoogen, F. H., van de Putte, L. B., and van Venrooij, W. J. (1998) Citrulline is an essential constituent of antigenic determinants recognized by rheumatoid arthritis-specific autoantibodies, *J. Clin. Invest. 101*, 273−281.
10. Girbal-Neuhauser, E., Durieux, J. J., Arnaud, M., Dalbon, P., Sebbag, M., Vincent, C., Simon, M., Senshu, T., Masson-Bessiere, C., Jolivet-Reynaud, C., Jolivet, M., and Serre, G. (1999) The epitopes targeted by the rheumatoid arthritis-associated antifilaggrin autoantibodies are posttranslationally generated on various sites of (pro)filaggrin by deimination of arginine residues, *J. Immunol. 162*, 585−594.
11. Masson-Bessiere, C., Sebbag, M., Durieux, J. J., Nogueira, L., Vincent, C., Girbal-Neuhauser, E., Durroux, R., Cantagrel, A., and Serre, G. (2000) In the rheumatoid pannus, anti-filaggrin autoantibodies are produced by local plasma cells and constitute a higher proportion of IgG than in synovial fluid and serum, *Clin. Exp. Immunol. 119*, 544−552.
12. Masson-Bessiere, C., Sebbag, M., Girbal-Neuhauser, E., Nogueira, L., Vincent, C., Senshu, T., and Serre, G. (2001) The major synovial targets of the rheumatoid arthritis-specific antifilaggrin autoantibodies are deiminated forms of the alpha- and beta-chains of fibrin, *J. Immunol. 166*, 4177−4184.
13. Baeten, D., Peene, I., Union, A., Meheus, L., Sebbag, M., Serre, G., Veys, E. M., and De Keyser, F. (2001) Specific presence of intracellular citrullinated proteins in rheumatoid arthritis synovium: relevance to antifilaggrin autoantibodies, *Arthritis Rheum. 44*, 2255−2262.
14. Schellekens, G. A., Visser, H., de Jong, B. A., van den Hoogen, F. H., Hazes, J. M., Breedveld, F. C., and van Venrooij, W. J. (2000) The diagnostic properties of rheumatoid arthritis antibodies recognizing a cyclic citrullinated peptide, *Arthritis Rheum. 43*, 155−163.
15. Vincent, C., Nogueira, L., Sebbag, M., Chapuy-Regaud, S., Arnaud, M., Letourneur, O., Rolland, D., Fournie, B., Cantagrel, A., Jolivet, M., and Serre, G. (2002) Detection of antibodies to deiminated recombinant rat filaggrin by enzyme-linked immunosorbent assay: a highly effective test for the diagnosis of rheumatoid arthritis, *Arthritis Rheum. 46*, 2051−2058.
16. Nogueira, L., Sebbag, M., Vincent, C., Arnaud, M., Fournie, B., Cantagrel, A., Jolivet, M., and Serre, G. (2001) Performance of two ELISAs for antifilaggrin autoantibodies, using either affinity purified or deiminated recombinant human filaggrin, in the diagnosis of rheumatoid arthritis, *Ann. Rheum. Dis. 60*, 882−887.
17. Hill, J. A., Southwood, S., Sette, A., Jevnikar, A. M., Bell, D. A., and Cairns, E. (2003) Cutting edge: the conversion of arginine to citrulline allows for a high-affinity peptide interaction with the rheumatoid arthritis-associated HLA-DRB1*0401 MHC class II molecule, *J. Immunol. 171*, 538−541.
18. Hagiwara, T., Nakashima, K., Hirano, H., Senshu, T., and Yamada, M. (2002) Deimination of arginine residues in nucleophosmin/B23 and histones in HL-60 granulocytes, *Biochem. Biophys. Res. Commun. 290*, 979−983.
19. Nakashima, K., Hagiwara, T., and Yamada, M. (2002) Nuclear localization of peptidylarginine deiminase V and histone deimination in granulocytes, *J. Biol. Chem. 277*, 49562−49568.
20. Wang, Y., Wysocka, J., Sayegh, J., Lee, Y. H., Perlin, J. R., Leonelli, L., Sonbuchner, L. S., McDonald, C. H., Cook, R. G., Dou, Y., Roeder, R. G., Clarke, S., Stallcup, M. R., Allis, C. D., and Coonrod, S. A. (2004) Human PAD4 Regulates histone arginine methylation levels via demethylimination, *Science 306*, 279−283.
21. Cuthbert, G. L., Daujat, S., Snowden, A. W., Erdjument-Bromage, H., Hagiwara, T., Yamada, M., Schneider, R., Gregory, P. D., Tempst, P., Bannister, A. J., and Kouzarides, T. (2004) Histone deimination antagonizes arginine methylation, *Cell 118*, 545−553.
22. Nakashima, K., Hagiwara, T., Ishigami, A., Nagata, S., Asaga, H., Kuramoto, M., Senshu, T., and Yamada, M. (1999) Molecular characterization of peptidylarginine deiminase in HL-60 cells induced by retinoic acid and 1alpha,25-dihydroxyvitamin D(3), *J. Biol. Chem. 274*, 27786−27792.
23. Fujisaki, M., and Sugawara, K. (1981) Properties of peptidylarginine deiminase from the epidermis of newborn rats, *J. Biochem. (Tokyo) 89*, 257−263.
24. Rogers, G. E., Harding, H. W., and Llewellyn-Smith, I. J. (1977) The origin of citrulline-containing proteins in the hair follicle and the chemical nature of trichohyalin, an intracellular precursor, *Biochim. Biophys. Acta 495*, 159−175.
25. Sugawara, K., Oikawa, Y., and Ouchi, T. (1982) Identification and properties of peptidylarginine deiminase from rabbit skeletal muscle, *J. Biochem. (Tokyo) 91*, 1065−1071.
26. Takahara, H., Oikawa, Y., and Sugawara, K. (1983) Purification and characterization of peptidylarginine deiminase from rabbit skeletal muscle, *J. Biochem. (Tokyo) 94*, 1945−1953.
27. Takahara, H., Okamoto, H., and Sugawara, K. (1986) Calcium-dependent properties of peptidylarginine deiminase from rabbit skeletal muscle, *Agric. Biol. Chem. 50*, 2899−2904.
28. Arita, K., Hashimoto, H., Shimizu, T., Nakashima, K., Yamada, M., and Sato, M. (2004) Structural basis for Ca^{2+}-induced activation of human PAD4, *Nat. Struct. Mol. Biol. 11*, 777−783.

29. Nakayama-Hamada, M., Suzuki, A., Kubota, K., Takazawa, T., Ohsaka, M., Kawaida, R., Ono, M., Kasuya, A., Furukawa, H., Yamada, R., and Yamamoto, K. (2005) Comparison of enzymatic properties between hPADI2 and hPADI4, *Biochem. Biophys. Res. Commun. 327*, 192−200.
30. Arita, K., Hashimoto, H., Shimizu, T., Yamada, M., and Sato, M. (2003) Crystallization and preliminary X-ray crystallographic analysis of human peptidylarginine deiminase V, *Acta Crystallogr. D59*, 2332−2333.
31. Knipp, M., and Vasak, M. (2000) A colorimetric 96-well microtiter plate assay for the determination of enzymatically formed citrulline, *Anal. Biochem. 286*, 257−264.
32. Sugawara, K., and Oyama, F. (1981) Fluorogenic reaction and specific microdetermination of ammonia, *J. Biochem. (Tokyo) 89*, 771−774.
33. Das, K., Butler, G. H., Kwiatkowski, V., Clark, A. D., Jr., Yadav, P., and Arnold, E. (2004) Crystal structures of arginine deiminase with covalent reaction intermediates; implications for catalytic mechanism, *Structure 12*, 657−667.
34. Lohse, D. L., Denu, J. M., Santoro, N., and Dixon, J. E. (1997) Roles of aspartic acid-181 and serine-222 in intermediate formation and hydrolysis of the mammalian protein-tyrosine-phosphatase PTP1, *Biochemistry 36*, 4568−4575.
35. Zhang, Z. Y., and Dixon, J. E. (1993) Active site labeling of the Yersinia protein tyrosine phosphatase: the determination of the pK_a of the active site cysteine and the function of the conserved histidine 402, *Biochemistry 32*, 9340−9345.
36. Humm, A., Fritsche, E., Steinbacher, S., and Huber, R. (1997) Crystal structure and mechanism of human L-arginine:glycine amidinotransferase: a mitochondrial enzyme involved in creatine biosynthesis, *EMBO J. 16*, 3373−3385.
37. Head, J. F., Mealy, T. R., McCormack, F. X., and Seaton, B. A. (2003) Crystal structure of trimeric carbohydrate recognition and neck domains of surfactant protein A, *J. Biol. Chem. 278*, 43254−43260.
38. Flaherty, K. M., Zozulya, S., Stryer, L., and McKay, D. B. (1993) Three-dimensional structure of recoverin, a calcium sensor in vision, *Cell 75*, 709−716.
39. Sixma, T. K., Terwisscha van Scheltinga, A. C., Kalk, K. H., Zhou, K., Wartna, E. S., and Hol, W. G. (1992) X-ray studies reveal lanthanide binding sites at the A/B5 interface of *E. coli* heat labile enterotoxin, *FEBS Lett. 297*, 179−182.
40. Fischle, W., Wang, Y., and Allis, C. D. (2003) Histone and chromatin cross-talk, *Curr. Opin. Cell Biol. 15*, 172−183.
41. Fischle, W., Wang, Y., and Allis, C. D. (2003) Binary switches and modification cassettes in histone biology and beyond, *Nature 425*, 475−479.
42. Schreiber, S. L., and Bernstein, B. E. (2002) Signaling network model of chromatin, *Cell 111*, 771−778.
43. Kuo, M. H., Brownell, J. E., Sobel, R. E., Ranalli, T. A., Cook, R. G., Edmondson, D. G., Roth, S. Y., and Allis, C. D. (1996) Transcription-linked acetylation by Gcn5p of histones H3 and H4 at specific lysines, *Nature 383*, 269−272.
44. Mizzen, C. A., Yang, X. J., Kokubo, T., Brownell, J. E., Bannister, A. J., Owen-Hughes, T., Workman, J., Wang, L., Berger, S. L., Kouzarides, T., Nakatani, Y., and Allis, C. D. (1996) The TAF(II)250 subunit of TFIID has histone acetyltransferase activity, *Cell 87*, 1261−1270.
45. Thompson, P. R., Kurooka, H., Nakatani, Y., and Cole, P. A. (2001) Transcriptional coactivator protein p300. Kinetic characterization of its histone acetyltransferase activity, *J. Biol. Chem. 276*, 33721−33729.
46. Hagiwara, T., Hidaka, Y., and Yamada, M. (2005) Deimination of histone H2A and H4 at arginine 3 in HL-60 granulocytes, *Biochemistry 44*, 5827−34.
47. Bannister, A. J., Schneider, R., and Kouzarides, T. (2002) Histone methylation: dynamic or static?, *Cell 109*, 801−806.
48. Ojima, I., Habus, I., Zhao, M., Zucco, M., Park, Y. H., Sun, C. M., and Brigaud, T. (1992) New and efficient approaches to the semisynthesis of taxol and its C-13 side chain analogs by means of beta-lactam synthon method., *Tetrahedron 48*, 6985−7012.
49. Lin, W. J., Gary, J. D., Yang, M. C., Clarke, S., and Herschman, H. R. (1996) The mammalian immediate-early TIS21 protein and the leukemia-associated BTG1 protein interact with a protein-arginine *N*-methyltransferase, *J. Biol. Chem. 271*, 15034−15044.
50. Strahl, B. D., Briggs, S. D., Brame, C. J., Caldwell, J. A., Koh, S. S., Ma, H., Cook, R. G., Shabanowitz, J., Hunt, D. F., Stallcup, M. R., and Allis, C. D. (2001) Methylation of histone H4 at arginine 3 occurs in vivo and is mediated by the nuclear receptor coactivator PRMT1, *Curr. Biol. 11*, 996−1000.
51. Kubota, K., Yoneyama-Takazawa, T., and Ichikawa, K. (2005) Determination of sites citrullinated by peptidylarginine deiminase using ^{18}O stable isotope labeling and mass spectrometry, *Rapid Commun. Mass Spectrom. 19*, 683−688.
52. Shirai, H., Blundell, T. L., and Mizuguchi, K. (2001) A novel superfamily of enzymes that catalyze the modification of guanidino groups, *Trends Biochem. Sci. 26*, 465−468.
53. Boehr, D. D., Thompson, P. R., and Wright, G. D. (2001) Molecular mechanism of aminoglycoside antibiotic kinase APH(3′)-IIIa. Roles of conserved active site residues, *J. Biol. Chem. 276*, 23929−23936.
54. Moldoveanu, T., Hosfield, C. M., Jia, Z., Elce, J. S., and Davies, P. L. (2001) Ca^{2+}-induced structural changes in rat m-calpain revealed by partial proteolysis, *Biochim. Biophys. Acta 1545*, 245−254.
55. Lewis, R. S. (2001) Calcium signaling mechanisms in T lymphocytes, *Annu. Rev. Immunol. 19*, 497−521.
56. Takahara, H., Tsuchida, M., Kusubata, M., Akutsu, K., Tagami, S., and Sugawara, K. (1989) Peptidylarginine deiminase of the mouse. Distribution, properties, and immunocytochemical localization, *J. Biol. Chem. 264*, 13361−13368.
57. Lau, O. D., Courtney, A. D., Vassilev, A., Marzilli, L. A., Cotter, R. J., Nakatani, Y., and Cole, P. A. (2000) p300/CBP-associated factor histone acetyltransferase processing of a peptide substrate. Kinetic analysis of the catalytic mechanism, *J. Biol. Chem. 275*, 21953-21959.
58. Sohn, J., Kristjansdottir, K., Safi, A., Parker, B., Kiburz, B., and Rudolph, J. (2004) Remote hot spots mediate protein substrate recognition for the Cdc25 phosphatase, *Proc. Natl. Acad. Sci. U.S.A. 101*, 16437−16441.
59. Schurter, B. T., Koh, S. S., Chen, D., Bunick, G. J., Harp, J. M., Hanson, B. L., Henschen-Edman, A., Mackay, D. R., Stallcup, M. R., and Aswad, D. W. (2001) Methylation of histone H3 by coactivator-associated arginine methyltransferase 1, *Biochemistry 40*, 5747−5756.

BI050292M